Wave attenuation over coastal salt marshes under storm surge conditions

Authors:

Iris Möller[1,2] *

Matthias Kudella[3]

Franziska Rupprecht[4]

Tom Spencer[1]

Maike Paul[3]

Bregje K. van Wesenbeeck[5]

Guido Wolters[5]

Kai Jensen[4]

Tjeerd J. Bouma[6]

Martin Miranda-Lange[3]

Stefan Schimmels[3]

*** corresponding author**

[1] Cambridge Coastal Research Unit, Department of Geography, University of Cambridge, Downing Place, Cambridge, CB2 3EN, UK; email: im10003@cam.ac.uk.
[2] Fitzwilliam College, Storey's Way, Cambridge CB3 0DG, UK.
[3] Forschungszentrum Küste (FZK), Merkurstr. 11, 30419 Hannover, Germany.
[4] Applied Plant Ecology, Biocenter Klein Flottbek, University of Hamburg, Ohnhorststr. 18, 22609 Hamburg, Germany.
[5] Deltares, Rotterdamseweg 185, 2629 HD Delft, NL.
[6] Yerseke Spatial Ecology, Netherlands Institute for Sea Research (NIOZ), Korringaweg 7, 4401 NT Yerseke, NL.

Coastal communities around the world face increasing risk from flooding as a result of rising sea level, increasing storminess, and land subsidence[1–2]. Salt marshes can act as natural buffer zones, providing protection from waves during storms[3–7]. However, the effectiveness of marshes in protecting the coastline during extreme events when water levels are at a maximum and waves are highest is poorly understood[8,9]. Here, we experimentally assess wave dissipation under storm surge conditions in a 300-meter-long wave flume tank that contains a transplanted section of natural salt marsh. We find that the presence of marsh vegetation causes considerable wave attenuation, even when water levels and waves are highest. From a comparison with experiments without vegetation, we estimate that up to 60% of observed wave reduction is attributed to vegetation. We also find that although waves progressively flatten and break vegetation stems and thereby reduce dissipation, the marsh substrate remained stable and resistant to surface erosion under all conditions. The effectiveness of storm wave dissipation and the resilience of tidal marshes even at extreme conditions suggests that salt marsh ecosystems can be a valuable component of coastal protection schemes.

Coastal margins are experiencing increased pressure from both physical environmental (sea level rise, increased storminess[10]) and human use (increased population densities, resource requirements[11]) perspectives. This has resulted in a re-evaluation of coastal flood and erosion risk reduction methods[5]. Natural coastal landforms, including sand dunes, mudflats and salt marshes, are now widely recognised as potential barriers to wave and tidal flow or as wave/tidal energy buffers[7,11–13]. The inclusion of such natural features into quantitative flood risk assessments, however, has been hampered by a lack of (i) empirical evidence for their capacity to act as wave dissipaters under extreme water level and wave conditions (when their coastal protection service is most required); and (ii) a quantitative understanding of their ability to survive those types of conditions[8,14–16].

Previous studies have suggested that wave dissipation over submerged salt marsh canopies is dependent on water depth and incident wave energy, and that hydrodynamic conditions may exist beyond which marshes lose their wave dissipating effect[6,17,18]. The existence of such conditions makes intuitive sense, as the orbital wave motion that is affected by the submerged vegetation canopy decreases with increasing depth and decreasing incident wave energy. Existing empirical studies of wave reduction over vegetated canopies have, however, been limited to low water depths (< 1 m) and low wave heights (< 0.3 m)[18,19].

Salt marsh resistance to wave impact is intricately connected to wave dissipation over salt marsh surfaces[20]. Under high energy conditions, dissipation of wave energy may be achieved by wave shoaling/breaking as well as removal of material (both plant and soil) from the marsh edge/surface, rather than only by drag from the vegetation canopy[19]. Existing evidence points to the stabilising effect of organic matter with respect to resistance of the marsh surface to erosion by waves from above (with contrasting evidence for roots increasing erosion on exposed marsh margins)[21]. Little is known, however, about the response of the marsh soil to extreme levels of wave impact, as might be experienced during a storm surge. The stability of the marsh surface under such conditions is critical to any assessment of its usefulness as part of coastal flood risk reduction schemes.

Here we present results of a unique large scale flume experiment with three key aims: to explore the dissipation of waves over a vegetated marsh canopy under storm conditions; to quantify the effect of vegetation on wave attenuation compared to the effects of a mowed platform; and to quantify the response of marsh vegetation and soil surface to incident wave energy.

Waves were generated in a 300-m-long, 5-m-wide, and 7-m-deep flume over a test section of almost 40m length consisting of a coherent patchwork of marsh blocks (Fig. 1a). Blocks were characterized by a mixed canopy of *Elymus athericus, Puccinellia maritima,* and *Atriplex prostrata*, typical of mid to high southern North Sea marsh communities (Fig. 1d). Whereas incident wave heights on salt marsh margins are limited by shallow inshore water depths and thus are generally low (<0.3 m), above-marsh water depths are known to reach or exceed 2 m, accompanied by wave heights (H_s) in excess of 0.8 m, during storms[19]. Tests were thus conducted for regular and irregular non-breaking waves of heights up to 0.9m in 2m water depth above the vegetated bed. There was no statistical difference between flume and field soil bulk density, stem diameter, and plant stem flexibility (Young's Modulus) (t-test; $p>0.05$) (see Table 1 and Supplementary Information for detail).

Results show a clear dissipation pattern, remarkably consistent between regular and irregular waves. For regular waves, wave energy dissipation over the 40m distance increased linearly from no dissipation in the case of waves with H=0.1m and T=1.5s to 19.5% reduction for H=0.3m and T=3.6s (Fig. 2a). For irregular waves, dissipation between 11.9 and 17.9% occurred for $H_{rms,0}$ of 0.2-0.4m (Fig. 2b). When incident wave heights increased beyond these levels, dissipation reduced to 13.8% for regular (H=0.6m, T=3.6s, Fig. 2a) and to 14.7% for irregular waves ($H_{rms,0}$=0.6m, T_p =4.0s, Fig. 2b), before increasing to 16.9% for the largest regular waves (H=0.7 and 0.9m; T=5.1 and 4.1s) and to 16.9% for the largest irregular waves ($H_{rms,0}$ =0.7m, T_p=6.2 s).

Dissipation over the mowed surface was significantly lower in all regular wave tests (t-test, $p<0.05$) (Fig. 2a) and irregular wave tests (Figure 2b). At (or just after) the point of maximum wave dissipation (H and $H_{rms,0}$ = 0.2-0.4 m), wave height reduction over the mowed section was lower than over the section with intact vegetation by a factor of 0.4. Thus it can be stated that the vegetation cover alone accounted for 60 % of wave height reduction (Fig. 2a,b). However, when $H_{rms,0}$ increased towards 0.6m, the vegetation cover accounted for only 40% of wave height dissipation (Fig. 2b).

Models of wave dissipation by vegetated beds commonly rely on knowledge of the drag coefficient C_D incorporated into a friction factor that takes account of vegetation stem density, height, and diameter. The complex nature of salt marsh vegetation precludes the *a priori* determination of C_D from simple plant metrics. Nevertheless, an exponential decay relationship between the stem Reynolds number Re_V and C_D of the form $C_D = a+(b/Re_V)^c$ has been found to exist for other vegetation types[22-24]. Here, Re_V is a function of wave orbital velocity and the vegetation stem diameter. We initially used our vegetation metrics (Table 1) and the C_D-Re_V relationship developed for seagrasses to predict dissipation for our experimental conditions[22]. Figure 2a, b clearly shows that our observed dissipation exceeded that predicted by a factor of 1.5-2.2 for regular and 2.6-3.2 for irregular waves. We then calculated C_D for each experimental run from observed dissipation and plant metrics. C_D decreased with increasing Reynolds numbers Re_V, confirming the established exponential relationship between Re_V and C_D ($r^2 \geq 0.97$), but with coefficients a, b, and c that differ from those of previous studies (see Supplementary Information).

Analysis of video footage showed that the reduction in dissipation for regular waves exceeding 0.3m in height was accompanied by a change in behaviour of the marsh vegetation. Under relatively low incident waves (H<0.3m; T<3.6s), the plants swayed and interacted with wave motion throughout the wave cycle (Figs. 2a and 3a). For larger waves (stronger currents), however, stems bent over to angles>50° during the forward wave motion, allowing the flow for part of the wave cycle to skim over, rather than travel through the vegetation, thus retaining energy and reducing dissipation (Figs. 2a and 3b).

Video observations confirmed that this flattening of the plants preceded the tendency for plant stems to fracture along lines of weakness that formed when stems folded over to high bending angles. Cumulatively, this breakage resulted in a loss of 31% (30 kg) of the total 98 kg of biomass after two days of runs under higher energy conditions (Fig. 2c). Such loss of plant material may then have contributed to the reduced dissipation (Fig. 2a, b). The soil surface remained remarkably stable, with an average lowering that was not significantly different from zero (4.4±10.4mm over the entire experiment). The trend for average surface lowering from one surface exposure to the next was greatest during the test runs with the largest waves, rather than during the test runs that resulted in the largest release of plant biomass (Fig. 2c).

Wave attenuation of > 80 % has been reported in the literature for distances of about 160m under low energy conditions[19]. The spatially non-linear nature of wave dissipation means that a conversion of this figure to units of per cent per metre makes little sense[4], but the evidence presented here shows that non-breaking wave dissipation can still reach 20% over a 40m distance even in water depths typically found during storm conditions. This contribution is generated not only by the marsh platform but also, and significantly, by the vegetation canopy. Moreover, we identify process transitions in wave dissipation across the submerged salt marsh surface, associated with specific incident wave energy levels. The spatio-temporal non-linearity in wave dissipation over coastal wetlands has been linked to, amongst other factors, variability in the characteristics of the vegetation cover (for example, flexibility[25]).The established general nature of the relationship between Re_V and C_D seems robust, even for storm conditions, but the coefficients describing this relationship in our experiment differ markedly from those established for lower energy conditions and different vegetation types[22-24]. For regular waves of around 0.6m height (Re_V of around 640), however, the model based on the empirical Re_V-C_D relationship leads to an over-prediction of dissipation (see Fig. 2a) that warrants further investigation. We thus call for a re-evaluation of existing wave dissipation models and urge the scientific community to develop more appropriate methods for the *a priori* quantification of vegetation-induced drag for a broader range of plant species and wave conditions. Ideally, such methods should be able to quantify drag directly from plant metrics and knowledge of the incident flow field. Furthermore, the high bending angle and repeated bending of vegetation under energetic conditions lead to plant breakage along lines of weakness and a loss of biomass, a process that needs to be adequately represented in models of marsh canopy growth/recovery after storm incidence.

The higher than expected rates of storm wave dissipation and the fact that marsh surfaces are able to withstand larger wave forces without substantial erosion effects increase their reliability as part of coastal defence schemes and shifts debates about marsh stability and resilience to those locations where the marsh profile is exposed. In such settings, lateral retreat (for example cliff undercutting/collapse on marsh fronts and channel widening)[26-28] may be enhanced by the presence of vegetation, for example when roots become exposed to wave impact[21]. The long-term balance between vertical and lateral marsh dynamics thus becomes a key area for further study[8,9].

The evidence presented here can serve as a validation data set for a new and improved representation of drag and friction effects in numerical models of wave dissipation and vegetation movement under storm conditions. It also supports the incorporation of salt marshes into coastal protection schemes, such as the Dutch 'building with nature' approach[5,11,20]. Any such schemes must carefully consider incident wave heights and water depths, alongside wave dissipation requirements and the ecological conditions necessary for the maintenance of a healthy vegetation canopy.

METHODS

Experimental set-up. Experiments were conducted in the Large Wave Flume (Grosser Wellenkanal, GWK) of Forschungszentrum Küste (FZK) in Hannover, Germany. The flume is the largest freely accessible wave tank in the world; it is 310m long, 5m wide and 7m deep. The vegetated test section of 39.44m length (about 180m^2) consisted of vegetated marsh blocks of 1.2m length, 0.8m width, and 0.3m depth, cut from a natural marsh on the mainland coast in Eastern Frisia, German Wadden Sea. The vegetated section was positioned on a 1.2m high sand base covered in geotextile at a distance of 108m from the wave paddle and illuminated to prevent plant deterioration when exposed. Adjacent to the front and rear end of the vegetated test section, a flat concrete surface and ramped concrete slope allowed waves to shoal (Fig. 1a).

Wave conditions and inundation schedule. The flume was filled with fresh water to 2.0m water depth above the vegetated soil surface and seven wave heights (H_{m0}: 0.1, 0.2, 0.3, 0.4, 0.6, 0.7 and 0.9 m) were simulated. Irregular waves ($N \geq 1000$) were generated using a JONSWAP spectrum with a peak enhancement factor of 3.3, followed by a regular wave run ($N \geq 100$). After each two days of tests, the flume was drained and exposed for at least 12h to allow plants to acquire oxygen. Tests were conducted with initially intact and then mowed vegetation to determine the effect of the vegetation as opposed to the topographic effect of the soil base.

Wave measurements. Sixteen wire wave gauges were deployed in sets of four (to enable reflection analysis at each location). Here we report analysed wave parameters from sets 2 and 4 that relate to the changes in wave characteristics over the full 40m of the vegetated section (see Fig. 1a,d). Wave gauges within each set were separated in the direction of wave travel by 2.07m (front two gauges), 1.55m (middle two), and 1.58m (back two).

Wave analysis. For the regular wave tests, the first 11 fully developed waves were found to be entirely unaffected by reflection from the flume end and were used to determine average wave height (H, from min-max water surface elevations) and period (T, from zero-upcrossing points). For irregular wave tests, the root-mean-square wave height in front of ($H_{rms,0}$) and behind ($H_{rms,1}$) the vegetated section was calculated after reflection analysis, as described in the Supplementary Information. Dissipation was analysed by comparing values at the last gauge of set 2 (3.02m in front of the vegetated section) and the first of set 4 (2.2m behind the vegetated section) and expressed as positive percentage of the wave height at the start of the section. If present, error bars indicate the standard deviation of the difference between the wave heights.

Wave dissipation model. Dalrymple et al.'s[29] model was used to compute the dissipation of regular waves and Mendez and Losadas'[30] model was applied to irregular waves over the 40 m long vegetated section x with H_0 ($H_{rms,0}$) incident wave height and H_1 ($H_{rms,1}$) damped wave height behind the section:

$$\frac{H_0 - H_1}{H_0} = \frac{\alpha x}{1 + \alpha x} \text{ (reg. waves)}, \qquad \frac{H_{rms,0} - H_{rms,1}}{H_{rms,0}} = \frac{\alpha x}{1 + \alpha x} \text{ (irreg. waves)}$$

In which

$$\alpha = A \frac{S_D}{S_S^2} C_D k \left[\frac{\sinh^3 kS_H + 3 \sinh kS_H}{\sinh kh (\sinh 2kh + 2kh)} \right]$$

Where

$A = 4/(9\pi)\, H_0$ for regular waves and $A = 2/(3\sqrt{\pi})\, H_{rms,0}$ for irregular waves, $k = 2\pi/L$ (L = wave length of peak period T_p), h = water depth, S_D = stem diameter, S_S = stem spacing, S_H = stem height as measured on the test section for *Elymus*, the dominant species (h = 2 m, S_D = 1.3 mm, S_S = 28.6 mm, S_H = 700 mm; Table 1).

The drag coefficient C_D was determined as a function of the Reynolds Number Re_v[22]:

$$C_D = -0.046 + \left(\frac{305.5}{Re_v}\right)^{0.977} \text{ (regular waves; } r^2 = 0.97\text{)}$$

$$C_D = 0.159 + \left(\frac{227.3}{Re_v}\right)^{1.615} \text{ (irregular waves; } r^2 = 0.99\text{)}$$

With

$$Re_v = U_{max} \frac{S_D}{v_k}$$

Where ν_k is the kinematic viscosity ($1 \times 10^{-6}\ m^2 s^{-1}$) and $U_{max} = f(H_0$ or $H_{rms,0}$ resp. and $T_p)$ the orbital velocity at the bottom in front of the vegetated section based on linear wave theory.

[For further details on field site, test section construction, wave analysis and methods used to analyse vegetation behaviour and damage as well as soil elevation change, refer to the Supplementary Information.]

Author contributions. IM, BvW, GW, TS, TB, SS, MK, MML, MP, and KJ designed the experiment. IM, FR, MK, MML, MP, TS, GW, and SS participated in the construction and running of the experiment. IM and MK conducted the wave data analysis with FR processing biomass and video information. IM processed the soil elevation data and wrote the initial manuscript. All authors contributed to and approved the final manuscript.

References:

1. Woodruff, J. D., Irish, J. L. & Camargo, S. J. Coastal flooding by tropical cyclones and sea-level rise. *Nature* **504,** 44–52 (2013).

2. Wong, P.P. *et al*. in *Climate Change 2014: Impacts, Adaptation, and Vulnerability. Part A: Global and Sectoral Aspects. Contribution of Working Group II to the Fifth Assessment Report of the Intergovernmental Panel on Climate Change* (eds Field, C.B. *et al*.) Ch. 5 (IPCC, Cambridge Univ. Press, 2014).

3. Loder, N. M., Irish, J. L., Cialone, M. A. & Wamsley, T. V. Sensitivity of hurricane surge to morphological parameters of coastal wetlands. *Estuar. Coast. Shelf Sci.* **84,** 625–636 (2009).

4. Koch, E. W. *et al.* Non-linearity in ecosystem services: temporal and spatial variability in coastal protection. *Front. Ecol. Environ.* **7,** 29–37 (2009).

5. Shepard, C. C., Crain, C. M. & Beck, M. W. The protective role of coastal marshes: a systematic review and meta-analysis. *PLoS One* **6,** e27374 (2011).

6. Gedan, K. B., Kirwan, M. L., Wolanski, E., Barbier, E. B. & Silliman, B. R. The present and future role of coastal wetland vegetation in protecting shorelines: answering recent challenges to the paradigm. *Clim. Change* **106,** 7–29 (2010).

7. Temmerman, S. *et al.* Ecosystem-based coastal defence in the face of global change. *Nature* **504,** 79–83 (2013).

8. Bouma, T. J. *et al.* Identifying knowledge gaps hampering application of intertidal habitats in coastal protection: Opportunities & steps to take. *Coast. Eng.* **87**, 147–157 (2014).

9. Kirwan, M. L. & Megonigal, J. P. Tidal wetland stability in the face of human impacts and sea-level rise. *Nature* **504,** 53–60 (2013).

10. Jones, H. P., Hole, D. G. & Zavaleta, E. S. Harnessing nature to help people adapt to climate change. *Nat. Clim. Chang.* **2,** 504–509 (2012).

11. Kabat, P. *et al.* Dutch coasts in transition. *Nat. Geosci.* **2,** 450–452 (2009).

12. Barbier, E. B. *et al.* The value of estuarine and coastal ecosystem services. *Ecol. Monogr.* **81,** 169–193 (2011).

13. US Army Corps of Engineers, Coastal Risk Reduction and Resilience (USACE, 2013); http://www.corpsclimate.us/docs/USACE_Coastal_Risk_Reduction_final_CWTS_2013-3.pdf

14. Spalding, M.D. *et al*. Coastal ecosystems: a critical element of risk reduction. *Conserv. Lett. **7***, 293-301 (2014).

15. Fagherazzi, S., Carniello, L., D'Alpaos, L. & Defina, A. Critical bifurcation of shallow microtidal landforms in tidal flats and salt marshes. *Proc. Natl. Acad. Sci. U. S. A.* **103,** 8337–8341 (2006).

16. Mariotti, G. & Fagherazzi, S. Critical width of tidal flats triggers marsh collapse in the absence of sea-level rise. *Proc. Natl. Acad. Sci. U. S. A.* **110,** 5353–5356 (2013).

17. Möller, I., Spencer, T., French, J. R., Leggett, D. J. & Dixon, M. Wave transformation over salt marshes: A field and numerical modelling study from North Norfolk, England. *Estuar. Coast. Shelf Sci.* **49,** 411–426 (1999).

18. Yang, S. L., Shi, B. W., Bouma, T. J., Ysebaert, T. & Luo, X. X. Wave attenuation at a salt marsh margin: A case study of an exposed coast on the Yangtze Estuary. *Estuaries and Coasts* **35,** 169–182 (2011).

19. Möller, I. & Spencer, T. Wave dissipation over macro-tidal saltmarshes : Effects of marsh edge typology and vegetation change. *J. Coast. Res.* **36,** 506–521 (2002).

20. Duarte, C. M., Losada, I. J., Hendriks, I. E., Mazarrasa, I. & Marbà, N. The role of coastal plant communities for climate change mitigation and adaptation. *Nat. Clim. Chang.* **3,** 961–968 (2013).

21. Feagin, R. A. *et al.* Does vegetation prevent wave erosion of salt marsh edges? *Proc. Natl. Acad. Sci. U. S. A.* **106,** 10109–10113 (2009).

22. Paul, M. & Amos, C. L. Spatial and seasonal variation in wave attenuation over *Zostera noltii*. *J. Geophys. Res*. **116**, C08019 (2011).

23. Mendez, F., Losada, I., & Losada, M. Hydrodynamics induced by wind waves in a vegetation field. *J. Geophys. Res*. **104, C8**, 18383-18396 (1999).

24. Kobayashi, N., Raichle, A., & Asano, T. Wave attenuation by vegetation. *J. Waterw. Port Coast. Ocean Eng.*, **119**, 30-48 (1993).

25. Mullarney, J. C. & Henderson, S. M. Wave-forced motion of submerged single-stem vegetation. *J. Geophys. Res.* **115,** C12061 (2010).

26. Howes, N. C. *et al.* Hurricane-induced failure of low salinity wetlands. *Proc. Natl. Acad. Sci. U.S.A.* **107,** 14014–14019 (2010).

27. Allen, J. R. L. Morphodynamics of Holocene salt marshes: A review sketch from the Atlantic and Southern North Sea coasts of Europe. *Quat. Sci. Rev.* **19**, 1155-1231 (2000).

28. Fagherazzi, S., Mariotti, G., Wiberg, P. L. & McGlathery, K. J. Marsh collapse does not require sea level rise. *Oceanography* **26,** 70–77 (2013).

29. Dalrymple, R. A., Kirby, J. T. & Hwang, P. A. Wave diffraction due to areas of energy dissipation. *J. Waterw. Port Coast. Ocean Eng*. **110** (1), 67-79 (1984).

30. Mendez, F. & Losada, I. An empirical model to estimate the propagation of random breaking and nonbreaking waves over vegetation fields. *Coast. Eng*. **51**(2), 103-119 (2004).

Correspondence and requests for materials should be addressed to Iris Möller at im10003@cam.ac.uk.

Acknowledgements. We thank all of the staff at the Grosser Wellenkanal as well as Ben Evans, James Tempest, Kostas Milonidis and Colin Edwards, Cambridge University, and Dennis Schulze, Hamburg University, for their invaluable logistical assistance, Fitzwilliam College for supporting the research time of IM, and Chris Rolfe, Cambridge University, for the soil analysis. The work described in this publication was supported by the European Community's 7th Framework Programme through the grant to the budget of the Integrating Activity HYDRALAB IV, Contract no. 261529 and a grant from The Isaac Newton Trust, Trinity College, Cambridge.

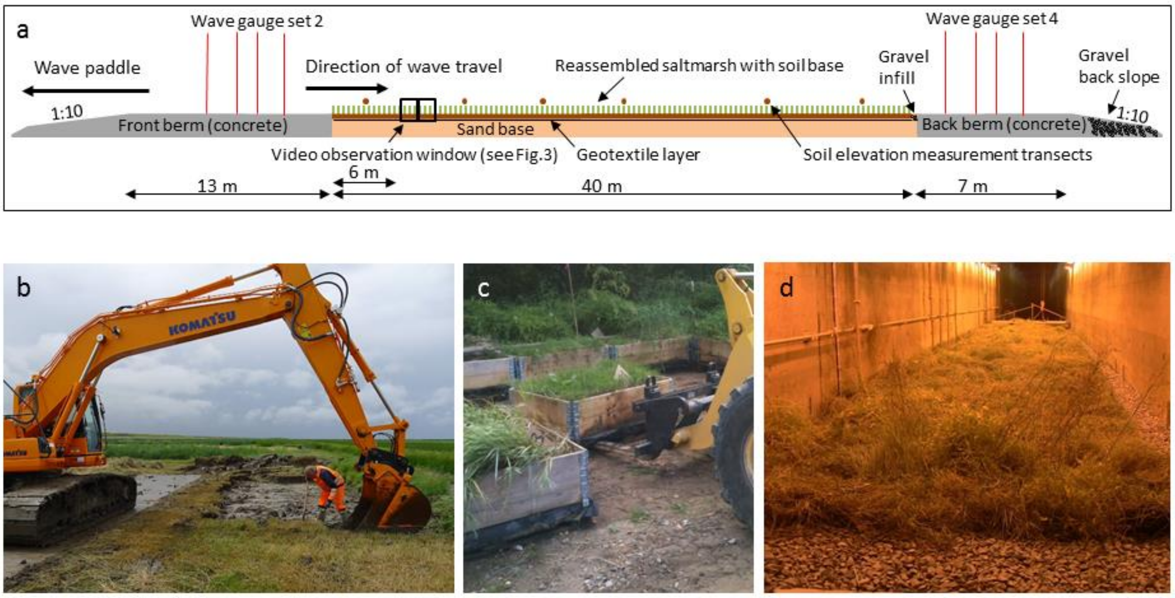

Figure 1 | Experimental set-up and photographs of excavation. a, General experimental set-up in the wave flume, with position of recording equipment relevant to reported results. **b,** Excavation of marsh blocks, northern German Wadden Sea (53°42.754 N, 07°52.963 E). **c,** Marsh blocks with *Elymus* vegetation cover prior to positioning in the flume test section. **d,** Reassembled salt marsh inside the 5-m-wide flume, looking towards the wave generator; lamps are mounted at about 3m above the soil surface.

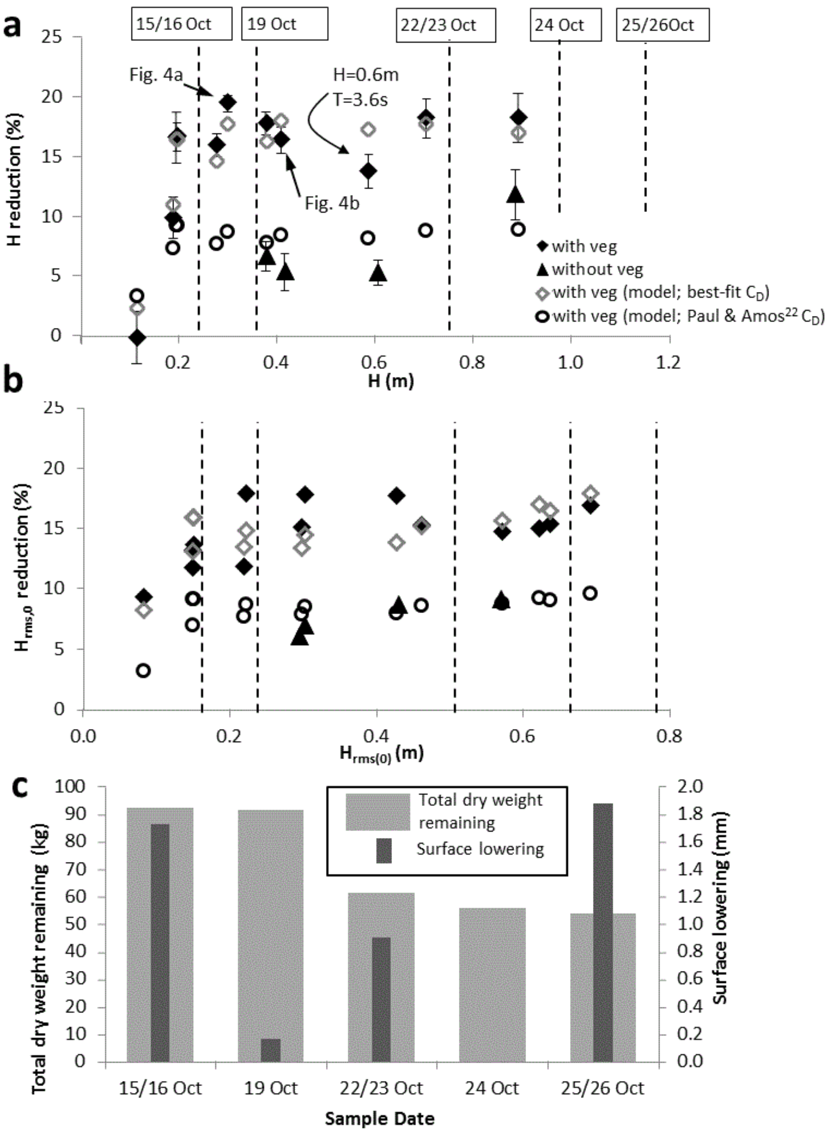

Figure 2 | Wave dissipation across 40 m of vegetated and mowed salt marsh. a,b Percentage reduction for regular waves (**a**: H) and irregular waves (**b**: $H_{rms,0}$), error bars in **a** refer to the mean ± 1 SD; filled diamonds/triangles refer to observed vegetated/mowed conditions, open diamonds and circles refer to modelled vegetated conditions using best-fit and ref.[22] C_D values respectively, vertical lines mark times of soil elevation and floating debris measurement (Fig. 2c) **c,** Plant biomass (light thick bars) remaining and mean surface elevation lowering (dark thin bars; standard error of ±10.4mm not shown).

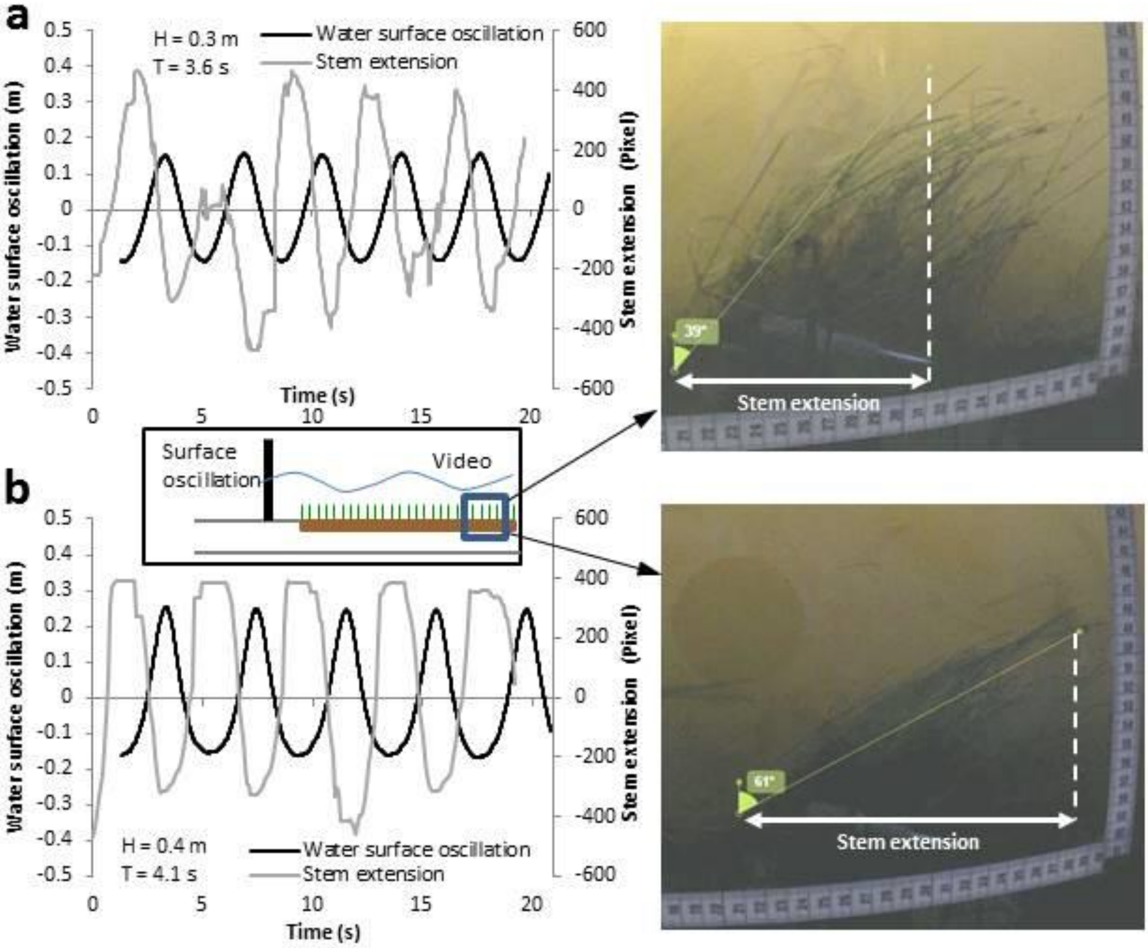

Figure 3 | *Puccinellia* plant canopy movement during wave motion. a,b Water level excursion (y-axis) and time-trace of horizontal stem extension (video pixel units; positive values in the direction of wave motion (white arrow in photographs)) under waves experiencing maximum dissipation (Fig. 2a) (**a**) and waves of greater height and period but experiencing lower dissipation (Fig. 2a) (**b**). A phase shift results from water level measurement occurring approximately 10m forward of video observations (see also experimental set-up in Fig. 1a). Lack of visibility in highly turbid water precluded analysis of conditions at H=0.6m, T=3.6s (Fig. 2a).

Table 1 | Plant stem flexibility (Young's Modulus), height, density, and diameter and soil bulk density at the field site where marsh blocks were extracted and in the flume immediately before the experimental runs (means ± one s.d.).

	Stem flexibility Young's bending modulus (MPa)		Stem height [mm]	Stem diameter [mm]		Stem density (number per 20 x 20 cm quadrat)		Dry soil bulk density (g cm^{-3})	
	Mean	**N**	**Mean**	**Mean**	**N**	**Mean**	**N**	**Mean**	**N**
***Puccinellia* (Flume)**	111.6 ± 66.3	17	220 ± 30	1.1 ± 0.3	17	-	-	0.6 ± 0.3	10
***Puccinellia* (Field)**	284.5 ± 369.1	17	-	1.2 ± 0.2	17	-	-	0.7 ± 0.5	20
***Elymus* (Flume)**	2,696.3 ± 1,963.8	18	700 ± 10	1.3 ± 0.3	18	49 ± 23	10	0.7 ± 1.0	20
***Elymus* (Field)**	2,514.6 ± 2,977.1	18	-	1.7 ± 0.4	18	68 ± 8	10	0.8 ± 0.7	20

Wave attenuation over coastal salt marshes under storm surge conditions

Iris Möller, Matthias Kudella, Franziska Rupprecht, Tom Spencer, Maike Paul, Bregje K. van Wesenbeeck, Guido Wolters, Kai Jensen, Tjeerd J. Bouma, Martin Miranda-Lange

SUPPLEMENTARY FIGURE, TABLE, AND METHODS

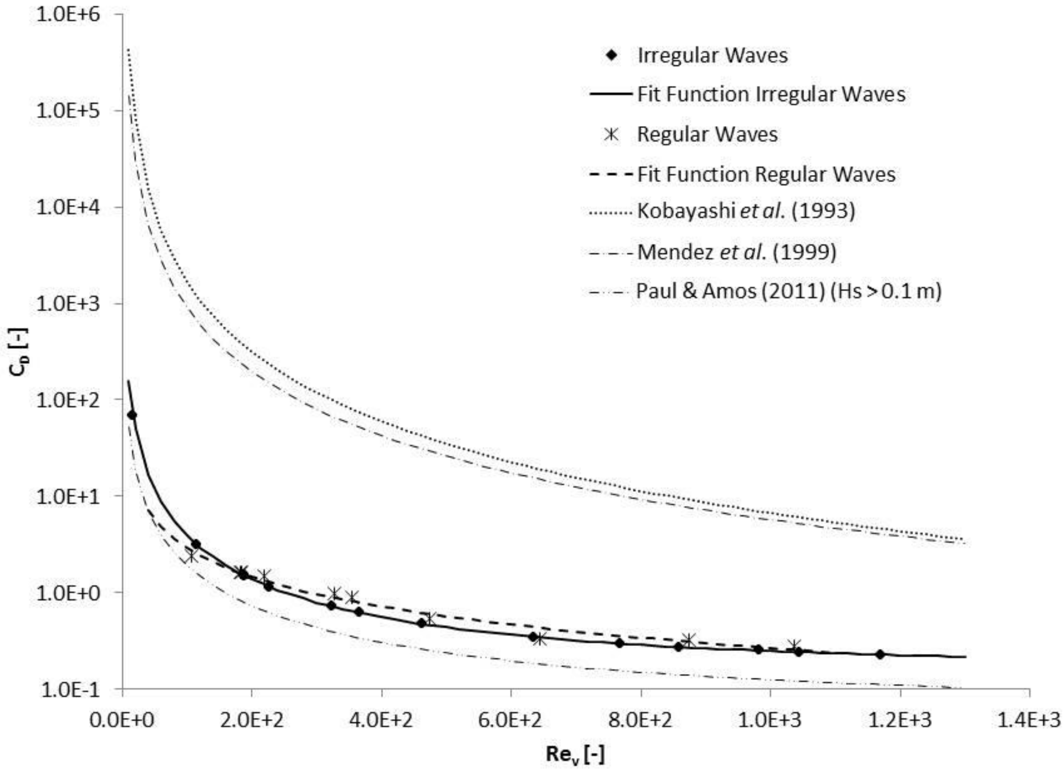

Figure 4 | Relationship between C_D and vegetation Reynolds number Re_V and best fit for regular and irregular waves. Also shown are the best fit lines of Kobayashi *et al.*[24], Mendez *et al.*[23], and Paul and Amos[22]. For best fit line equation and coefficients, see methods and Table 2.

Table 2 | Coefficients of the exponential decay function relating C_D to Re_V as determined in previous studies and this experiment.

Study	Vegetation type	a	b	c
Kobayashi *et al*. (1993)[24] (data from Asano *et al*. (1988))	Kelp	0.08	2200	2.40
Mendez *et al*. (1999)[23]	Kelp (rigid)	0.08	2200	2.20
	Kelp (swaying)	0.40	4600	2.90
Paul and Amos (2011)[22]	Seagrass	0.06	153	1.45
This experiment	Salt marsh (regular waves)	-0.05	306	0.98
	Salt marsh (irregular waves)	0.16	227	1.62

SUPPLEMENTARY METHODS

Field site. The vegetated marsh blocks were cut from a natural marsh on the mainland coast in Eastern Frisia, German Wadden Sea (53°42.754 N; 07°52.963 E) in June 2012. Blocks were lifted mechanically and placed on a wooden pallet, lined with a plastic sheet covered by a layer of geotextile. The experiment could not be scheduled prior to autumn 2013 and marsh blocks were stored outdoors in appropriate temperature/moisture conditions and with fences to control for herbivory for 14 months. For marsh construction in the flume, individual blocks were separated from their wooden base, lowered into position and keyed to neighbouring blocks using a marsh clay sealant.

Experimental test section illumination. Illumination of plants on the test section was achieved by 60 flume wall-mounted lamps (GE 750W 400V PSL or equivalent).

Wave analysis. For irregular wave tests, time-series of water level fluctuations were used to determine incident and reflected waves using the standard three-gauge method of Mansard and Funke[31]. After applying a low pass filter at $3.3f_p$ (with f_p = peak frequency) and a high pass filter at $f_p/2.1$, incident spectra were used to compute the peak wave period (T_p). After a reverse FFT of the incident spectrum the root-mean-square wave height in front of ($H_{rms,0}$) and behind ($H_{rms,1}$) the vegetated section was calculated according to $H_{rms} = \sqrt{\frac{1}{N}\sum_{i=1}^{N} H_i^2}$, where N is the number of incident waves and H_i the individual waves in the time series of incident waves.

Vegetation behaviour and damage. The Youngs' Modulus was measured according to the method described in Miler *et al*.[32]. Bending tests were performed with a ZWICK 1120 mechanical testing machine using a 100 N load cell (resolution 0.012 N) and a 1000 N load cell (resolution 0.12 N); Zwick GmbH & Co. KG, Ulm, Germany). Videography from behind lateral observation windows was used to record plant movement at a frequency of 10 Hz (Fig. 1a). Movement of plant stems was analysed using frame-by-frame tracking of stems[23], using 'Kinovea' video analysis software. All floating organic debris was removed using a net (1 cm mesh size) when necessary and total dry weight was determined.

Soil elevation measurements. Soil elevation was measured from an access platform, lowered into six cross-flume positions, whenever the vegetated section was drained (Fig. 1a). The surface of the platform was approximately 30 cm above the soil base and temporarily locked into fixed basal slots, to within 1 mm accuracy. Soil surface elevations were determined with respect to a horizontal bar fixed to the platform. Pins were lowered vertically onto the soil surface every 20 cm along the bar to determine soil surface elevation to millimetre accuracy.

31. Mansard, E. P. D. & Funke, E. R. The measurement of incident and reflected spectra using a least squares method. *Proc. 17th Coast. Eng. Conf. Vol 1* 154–172 (American Society of Civil Engineers, 1980).

32. Miler, O., Albayrak, I., Nikora, V. & O'Hare, M. Biomechanical properties of aquatic plants and their effects on plant-flow interactions in streams and rivers. Aquat. Sci. **74**, 31-44